

# Numerical and Experimental Investigations of Heat Transfer Enhancement in a Duct Heater with Different Areas of Vortex Generators

**Afrah Turki Awad**

Mech. Eng. Dep. University of Leeds  
Leeds- United Kingdom  
[af\\_ta88@yahoo.com](mailto:af_ta88@yahoo.com)

**Kutaeba J. M. Al-Khishali**

Mech. Eng. Dep. University of Philadelphia  
Amman-Jordan  
[Kutaibaal\\_khishali@yahoo.com](mailto:Kutaibaal_khishali@yahoo.com)

## Abstract:

Numerical and experimental investigations were carried out on the effect of the vortex generators on the flow field and heat transfer from duct heaters. The flow Reynolds number ranging from  $32000 < Re < 83000$  with a constant heat flux of  $43.09426 \text{ KW/m}^2$ .

In the numerical investigation, Fluent package (6.3) was used to solve the steady, (3-D), continuity, momentum and energy equations where the standard (k-ε) model was used to remedy the turbulent effects. Theoretical results show that the presence of VGs would save 27% of heaters power. The effects of two areas of VGs were looked at a small circle cross section

vortex generator (SCCSVG) and a big circle cross section vortex generator (BCCSVG) of similar shapes (where  $\frac{R_{BCCSVG}}{R_{SCCSVG}} = 1.5$ ).

The experimental results showed that there were an enhancement in heat transfer with the presence of VGs and heat transfer depends on VGs' areas. The BCCSVG was the better one of enhancing heat transfer by (2.76%-4.11%). Additionally, the increase of area of VGs, number of rows for VGs and the distance between each two rows of VGs and the heaters are the most effective parameters in improving the performance of heat transfer.

**Keywords:** VGs, heat transfer

## Nomenclature

Symbol	Description
d	Diameter of heater, cm
$D_h$	Hydraulic diameter of duct, m
$R_{VGs}$	Radius of VGs, cm
h	Heat transfer coefficient, $W/m^2 \cdot K$
I	Current output from heaters, Amp.
k	Thermal conductivity, $W/m \cdot K$
N	Number of heaters
$R_{BCCSVG}$	Radius of BCCSVG, cm
$R_{SCCSVG}$	Radius of SCCSVG, cm
$\overline{T_b}$	Bulk air temperature, °C
$T_f$	Film air temperature, °C
$T_h$	Heater surface temperature, °C
$u_i$	Axial velocity at tube entrance, m/s
V	Voltage output from heaters, Volt.
x	Length of heater, cm
$X_d$	The distance between VGs row and heaters row, cm
$\Delta T$	Difference between $T_h$ and $\overline{T_b}$ , °C
$\Delta p$	Air pressure drop, Pa
<b>Subscript Symbols</b>	<b>Description</b>
BCCSVG	Big circle cross section vortex generators.
d	Distance
h	Hydraulic
i	Inlet
r	Ratio
SCCSVG	small circle cross section vortex generators.

Abbreviation	Description
LVGs	Longitudinal Vortex Generators
VGs	Vortex Generators
WVGs	Winglet Vortex Generators

## 1. Introduction :

In recent years, energy and material saving considerations have promoted an expansion of efforts aimed at producing more efficient heat exchanger equipment through the augmentation of heat transfer. The potentials of heat transfer in engineering applications are high. Where a large number of industrial applications use the heat and mass transfer phenomena such as chemical, petrochemical, biomedical, air-conditioning equipment, etc. The use of enhanced surfaces allows the designer to increase the heat duty for a given exchanger, usually with pressure drop penalty, or to reduce the size of heat exchanger for a given heat duty. Variety of different techniques that employed for heat transfer process generally referred to the enhancement goal [1].

The heat transfer enhancement can be obtained by making or adding some additives such as: fins, wings, ribs, rods, winglets (half-wing vertical to the fin plane), or any interrupted surfaces or porous surfaces to improve convection. One of the most common methods of enhanced heat transfer is by using vortex generators. A vortex generator is a technique that holds promise in air-side heat transfer enhancement [2].

These enhancement techniques can be classified into two main categories: active and passive techniques. The former consist of mechanical devices able to modify directly the boundary layer structure (suction or injection of fluid, fluid and surface vibrations, jet impingement, etc); the latter are static devices as perturbation grids, winglets, surface ribs or grooves, placed upstream the heated body in order to increase perturbations and turbulence intensity in the flow stream [3]. These passive schemes promote higher heat transfer coefficients. In the case of active techniques, the addition of external power essentially facilitates the desired flow modification and the concomitant improvement in the rate of heat transfer [4].

## 2. Brief review of previous work:

The numerical simulation by Fluent program and the experimental study had been performed by [5] to examine the local and mean heat transfer performance of circular and elliptical tubes with vortex-generator winglets. The local heat transfer results clearly indicate areas of heat transfer enhancement associated with both the primary vortex and the corner, horseshoe-type

vortices produced by each winglet. Evaluation of mean fin-surface heat transfer coefficients indicated that the addition of the single winglet pair to the oval-tube geometry yielded significant heat transfer enhancement, averaging 38% higher than the oval-tube, no-winglet case. Highest mean heat transfer coefficients were observed for the case of a circular tube plus winglets with the winglets located on the downstream side of the cylinder, oriented at a 45° angle to the flow.

In order to clarify the effect of winglet pair on heat transfer enhancement than the single winglet by [6] and resulted that the enhancement in heat transfer due to a pair of winglets is almost twice that due to a single winglet, a winglet of finite thickness is marginally superior to the idealized zero thickness winglet. It is surmised that the finite thickness of winglet provides more cross sectional area for energy transfer from the bottom plate than an increase in heat transfer.

Examined the heat transfer and friction loss behaviors for airflow through a constant heat flux channel fitted with ten pairs of rectangular winglets turbulators by [7], to investigated the effects of delta winglet arrangements by pointing upstream and pointing downstream of the flow and effects of attack angle on heat transfer and friction loss in the channel. Then concluded that the use of the rectangular WVGs provides significantly higher heat transfer rate and friction loss than the smooth wall channel heater. The larger the attack angle value leads to higher heat transfer rate and friction loss than the lower one.

The aim of present study is to investigate turbulent flows in rectangular ducts using two different areas of VGs and different location, to know the effect of these small bodies on flow and heat transfer characteristics.

A rig is to be designed the numerical investigation then applies this design in the experimental part for a range of Reynolds number (32000-83000). Also a correlation between the Nusselt number and Reynolds number is to be found.

## 3. Numerical method:

A commercial computational fluid dynamics code (FLUENT) is used to simulate the flow field. Non-uniform structured meshes are generated by Gambit program in which the grids near the walls are chosen to be a fine one. Second order upwind scheme is used to discretize the convective term of the governing equations, and a central difference scheme is employed for the diffusion term.

The Fluent solver is based on the finite volume method. This law is expressed in terms of partial differential equation which is discretized with finite volume based technique. The solution to the turbulent problem then revolves around the solution of the turbulent viscosity. The turbulent viscosity is calculated as a function of the turbulence model, kinetic energy (K) and its dissipation rate ( $\epsilon$ ). The empirical constant is in the (K- $\epsilon$ ) models. The discretized conservation is solved iteratively. A number of iterations are usually required to reach a converged solution.

The choice of the mesh type to be use by Gambit program will depend on the application. For the problems which involve complex geometries, the creation of structured or block-structured grids (consisting of hexahedron cells) can be extremely time-consuming, if not impossible. The setup time is, therefore, the major motivation for using unstructured grids employing tetrahedron cells.

The range of length scales of the flow is large and a tetrahedron mesh can often be created with far fewer cells than the equivalent mesh consisting of hexahedron cells.

This is because a tetrahedron mesh allows cells to be clustered in selected regions of the flow domain as shown in fig.(1) at the heaters and vortex generators region.

Whereas, structured hexahedron meshes will generally force cells to be placed in regions where they are not needed.

This is the reason behind the choice of unstructured tetrahedron meshes in the current study.

**4. Configurations and Verification:**

Two cases were studied, the BCCSVG and SCCSVG of a similar shape with different areas, where the radius ratio is ( $\frac{R_{BCCSVG}}{R_{SCCSVG}} = 1.5$ ) in order to study the effect of increasing areas of VGs on the heat transfer enhancement, with 1 row of VGs (VGs before heaters set) and 3rows of VGs (VGs before and in-between heaters set). There are two selected cases to study the effect of distance between VGs rows and heaters rows, which considered as  $X_d=1\text{cm}$  and  $X_d=2\text{cm}$ .The details of VGs number and dimensions as shown in table (1).

**Table 1:** the details of VGs’ dimensions and numbers, where the spaces between each two VGs. in the same row, in z direction, is 3 cm

VGs. type	$R_{VGs}$ (cm)	Area( $\text{cm}^2$ )	Arranged no. of VGs. before heaters set	Arranged no. of VGs. before and in-between heaters set
BCCS VG	1.2	4.52	(28) numbers of BCCSVG	(28x3) numbers of BCCSVG
SCCS VG	0.8	2	(28) numbers of SCCSVG	(28x3) numbers of SCCSVG

The most beneficial of Fluent and Gambit programs were to select the suitable design for the test section (contained heaters and VGs). After many runs on the program investigating the number of heaters, the arrangement of heaters rows and the distances between each of the three rows of heaters {heaters bank},in a staggered arrangement, that gives a better enhancement.

Also the arrangement of VGs, VGs areas (as BCCSVG or SCCSVG), the arrangement of VGs considering the effect of distances between VGs rows and heaters rows as ( $X_d=1\text{cm}$  or  $X_d=2\text{cm}$ ). Gambit and Fluent program were used and run over these different possible cases to design the experimental rig.

**5. Apparatus and procedure:**

In the apparatus set up, the 11 heaters of 0.65cm in diameter of 30cm long in a wooden duct, the amount of power generated from heaters was controlled by the voltage regulator to give the required heat. The air velocities from the blower, measured by an anemometer device, were adjusted by varying the throttle valve to get the required values of Reynolds numbers. Fig. (2) to show the experimental rig and fig.(3-a) to show the SCCSVG while the fig.(3-b) to show the BCCSVG that used during the experimental work. For each test run, it was necessary to record the data of temperature (at different locations as shown in fig. (2)), air velocity and pressure drop. The characteristics of the Nusselt numbers, effectiveness and the Reynolds numbers were based on the film temperature calculated for the heater temperature and the averaged air temperature. Air is used as the working fluid. All properties calculated as:

$$T_f = \frac{(T_h + T_b)}{2}$$

Where

$$\bar{T}_b = \frac{T_{air\ in} + T_{air\ out}}{2}$$

Heaters power is calculated according to the following relation:

$$q_{heaters} = VI \quad \dots (1)$$

And heat flux is given by:

$$q_{air} = q_{conv.} = h A \Delta T \quad \dots (2)$$

Then heat transfer coefficient is calculated according to:

$$h = \frac{q_{air}}{A.(\Delta T)} \quad \dots (3)$$

Note that:

$$\Delta T = T_h - \overline{T_b} \quad \dots (4)$$

And the area of heaters was calculated by:

$$A = \pi * N * d * x$$

Nusselt number defined as:

$$Nu = \frac{h.D_h}{k} \quad \dots (5)$$

The Reynolds number is given by

$$Re = \frac{\rho.u_i .D_h}{\mu} \quad \dots (6)$$

## 6. Results and Discussion:

### 6.1 Numerical Result:

Numerical investigations for a flow velocity of (4, 8 and 10 m/s) are carried out. The contours of total temperature distributions are shown fig. (4 to 21) for velocity of 4m/s and 10m/s where the effect of VGs presence before or before and between heaters set for different areas of VGs (BCCSVG or SCCSVG), and the distance between VGs rows and heaters rows as  $X_d=1\text{cm}$  or  $X_d=2\text{cm}$ , on heat transfer performance is compared with the case of without VGs. The eddies formation are differ at different area of VGs as shown in the fig. (4 to 21).

The vortex is a manifestation of the vortices generated in the separated shear layer at the leading edge of each VGs and its interaction with the mean secondary flow from the lower to the upper side wall. The vortex core is small and located in the close vicinity of the VGs at its origin near the lower side wall. The development and growth of the vortex can be clearly seen behind each VGs, they move in line with the secondary flow from the lower to the upper wall and impinge on the upper wall, enhancing the heat transfer in that region.

For all previous cases, eddies with 3rows or 1row of VGs a longer shows life time than the case of no VGs, notice the shape of horseshoe vortices around heaters and the longitudinal vortices due to VGs presence and their effect on heat transfer performance.

It clearly shown that the longitudinal vortices lead to the deformation of the temperature profiles. The variations of temperature profile tell us that the VGs are spreading gradually and leading to the mixing of fluid. The temperature boundary layer becomes thinner in the areas where the secondary flow washes upon the wall while the temperature boundary layer becomes thicker in the areas where the secondary flow is away from the wall [8]. A similar trend is produced in the present work.

The heat dissipates to the upper wall of duct due to the effect of bouncy force on heat transfer.

Fluent predication shows that VGs present shows an energy save, also cooling the test section and produce a better mixing, while the absence of VGs, more heat flux power are needed (about 27%) than that when VGs are present.

The eddies formed for all cases considered would die out quickly with the increasing of velocity (Reynolds number).The distance between VGs rows and heaters set with ( $X_d=2\text{cm}$ ) was better than ( $X_d=1\text{cm}$ ) because eddies would have a longer life time.

As shown in the fig. (4 to 21) of total temperature distribution, eddies with 3rows of VGs have a longer life time than the case of 1row of VGs.

### 6.2 The experimental results

The experimental study has been carried out at different Reynolds numbers based on the hydraulic diameter of the duct for different arrangement, distances, shapes and areas of VGs, respectively.

The location of the VGs was varied according to the longitudinal distance  $X_d$ .In the experimental work, velocities of (8m/s and 10m/s) and also 4m/s were chosen in order to compare high flow(high Reynolds number) with a minimum flow (minimum Reynolds number).

All cases studied were under turbulent flow conditions.

#### 6.2.1 Temperature distribution

The temperature results starting point is from the first row of heaters. See fig. (2) for thermocouples locations. Fig.(22 to 29) shows the temperature verification along the duct for a flow without VGs and with the presence of VGs for a velocity of (4 and 10 m/s). The maximum temperature is for without VGs (due to undisputed heat in the test section) followed by the SCCSVG which is higher than that of the BCCSVG for a velocity of 10m/s. But of the case of velocity=4m/s, for case of 3rows of VGs at a distance of  $X_d=1\text{ cm}$  and the case of 1 row of VGs of the two cases  $X_d=1\text{cm}$  and  $X_d=2\text{cm}$ , the maximum temperature is for without VGs followed by the BCCSVG which is higher than that of the SCCSVG.

The effect of outlet temperatures and the temperatures curves shapes for all cases of 1row of VGs and 3rows of VGs with  $X_d=1\text{cm}$  and  $X_d=2\text{cm}$  seems to have an identical trends with BCCSVG as the highest among all followed by the SCCSVG than that of without VGs.

All curves show a similar trend physically but BCCSVG is the best one due to high outlet temperatures which lead to higher Nusselt number.

### 6.2.2 Nusselt number distributions

The experimental calculation of Nusselt number variation with Reynolds number, the heaters without VGs with either BCCSVG or SCCSVG prior or prior and between the heaters are shown in fig. (30 to 32).

All cases have the same trend with BCCSVG as the highest among all followed by the SCCSVG higher than without VGs as shown in fig. (30).

Fig.(31 to 32) shows that 3rows of BCCSVG better than 1 row of BCCSVG while these two are higher than that of the case without VGs for  $X_d=1\text{cm}$  and  $X_d=2\text{cm}$ , respectively. The best distance between each two rows of heaters and VGs is  $X_d=2\text{cm}$  which show higher values of Nusselt number.

As observed from fig. (31 to 32) the Nusselt number increases from low Reynolds number to high Reynolds number as expected, this result due to the formation of a horseshoe vortex system that consists of two counter-rotating longitudinal vortices which improves heat convection. Which is the heat transfer caused by the horseshoe or necklace vortices around the tube.

Enhancement of Nusselt number associated with the corner vortex system is visible for the VGs which are far from the tubes. The corner vortices of the nearer VGs coalesce with the main vortices of other VGs.

As shown in fig. (30) Nusselt number increases by inserting BCCSVG or SCCSVG.

The wave-like distribution of the local Nusselt number in the cross-flow direction is found. The heat transfer is enhanced near the centerline of the heater wall due to the relatively higher velocity.

The heat transfer is enhanced due to the strong longitudinal vortices generated by the presence of the LVGs the value of Nusselt decreases along the flow direction near the centerline and far from the centerline, the value of Nu reverses. This is because the velocity near the centerline reduces and the longitudinal vortices generate behind the LVGs far from the centerline and the distance between the cores of the vortices increases along the flow direction [9], this shows a similar trend with the present work.

Comparing the present work with [11] shown in fig.(33), which shows a similar trend with the present work. Where the range of Reynolds number in [11] is contained in the range of Reynolds number in the present work.

### 6.2.3 Effectiveness distributions

Values of effectiveness calculated according to:

$$\varepsilon = \frac{Nu_{with\ VGs} - Nu_{without\ VGs}}{Nu_{without\ VGs}} * 100\% \quad \dots (7)$$

Fig. (34 to 35) show the experimental calculation of the effectiveness variation with Reynolds number. They show the effectiveness for the heaters with VGs with either BCCSVG or SCCSVG prior and between heaters.

All of these figures have the same trend with BCCSVG shows to be higher than SCCSVG. From these figures notice the increase from a low Reynolds number (at velocity 4m/s) to higher Reynolds number (at velocity 8m/s) then decrease at highest Reynolds number (at velocity 10m/s).

Resulted that all of the 3 rows of VGs have better integrated flow and heat transfer characteristics than those of 1row of VGs this is because increasing number of VGs enhanced heat transfer. Also the ( $X_d=2\text{cm}$ ) is better than ( $X_d=1\text{cm}$ ) refer to elongated eddies life time between the VGs and heater, as shown in fig. (34 to 35).

From the above results the beneficial of adding VGs is to add turbulence to the air, where the heat is convected from the heaters and transferred convectively into the fluid flow in the flow passage, with losses to the wall of duct and to cool the test section.

### 6.2.4 Pressure drop distributions

During the tests pressure drop values were calculated at different velocity. Pressure drop percentage, compared between two cases of with VGs and without VGs, was calculated according to :

$$\Delta p_{ratio} = \frac{\Delta p_{with\ VGs} - \Delta p_{without\ VGs}}{\Delta p_{without\ VGs}} * 100\% \quad \dots (8)$$

And the results of the above equation is as follows: For 1row of VGs at  $X_d=1\text{cm}$  the values of pressure ratio are: ( for BCCSVG (87.91-157.79)% ) and (for SCCSVG (88.07-125.56)% ), for 1row of VGs at  $X_d=2\text{cm}$  the values of pressure ratio are: ((for BCCSVG (87.95-125.53)% and (for SCCSVG (87.99-93.303)% ) , 3rows of VGs at  $X_d=1\text{cm}$  the values of pressure ratio are: ((for BCCSVG (400-133.33)% ) and (for SCCSVG (300-100)%)) and for 3rows of VGs at  $X_d=2\text{cm}$  the values of pressure ratio are: ( for BCCSVG (500-200)% and (for SCCSVG (400-166.7)% ).

The pressure drop for BCCSVG have a large values than SCCSVG (due to higher surface area and the action caused by the reverse flow), also noticed that the increase of  $X_d$  between the rows of VGs and heater rows led to the increase of pressure drop.

Moreover, the pressure drop has a high possibility of occurring by the interaction of the

pressure forces with inertial forces in the boundary layer. It is clear that the addition of BCCSVG increase both the outlet temperature and pressure drop in the duct heater flow.

The distance ( $X_d=2\text{cm}$ ) between rows of VGs and rows of heater is better than ( $X_d=1\text{cm}$ ) because the increase of  $X_d$  lead to high turbulence formed and a longer life time of eddies.

**7. Comparison between Experimental and Numerical results:-**

The BCCSVG with  $X_d=2\text{cm}$  and for 3rows of VGs is compared with the case of without VGs, this shows that the numerical result from Fluent have the same trend as experimental curves as shown in fig. (36 to 38) for all cases such (BCCSVG at  $X_d=2\text{ cm}$  with either 3 rows of BCCSVG or 1row of BCCSVG and without VGs) the results curve would be of the same trend.

There is no big difference between experimental and numerical solution but these little difference are due to the uncertainty of devices used during experimental that lead to an experimental error.

**8. Correlation Equations with an error of the 2.6% for all the equations below are:**

For without VGs. :  

$$\text{Nu}=2.28*\text{Re}^{0.431}*\text{Pr}^{0.333} \quad \dots (9)$$

For 1row of VGs. :  

$$\text{Nu}=3.64*\text{Re}^{0.391}*\text{Pr}^{0.333} \quad \dots (10)$$

For 3rows of VGs. :  

$$\text{Nu} = 2.017 * \text{Re}^{0.446} * \text{Pr}^{0.333} \quad \dots (11)$$

The ratio of Nu with VGs. and Nu without VGs. is:

For 1 row of VGs. :  

$$\text{Nu}/\text{Nu}_0=1.596*\text{Re}^{0.9072} \quad \dots (12)$$

For 3 rows of VGs. :  

$$\text{Nu}/\text{Nu}_0=0.8846*\text{Re}^{1.035} \quad \dots (13)$$

**9. Conclusions**

This work has reached to the following conclusions:

1. Increasing the distances between heaters would decrease heat transfer enhancement, due to the reduction of the wake intensity generated.
2. VGs presence, shape, area, distance and distribution had an enhanced heat transfer coefficient, outlet temperatures and pressure drop
3. The BCCSVG is better than SCCSVG for enhancing heat transfer (comparing the same shapes of different areas).

4. Heat transfer increases when the distance of VGs before or before and in-between heaters increase from  $X_d=1\text{cm}$  to  $X_d=2\text{cm}$ .

5. The heat transfer enhancement Effectiveness ( $\epsilon$ ) increases with increasing the number of VGs rows. The maximum value for effectiveness {heat transfer enhanced} is in the case of 3rows of VGs at  $X_d=2\text{cm}$  , where the heat transfer around heaters was enhanced by(2.76-4.11)% using BCCSVG and it was enhanced by (2.186-3.75)% using SCCSVG .

6. Nusselt number increases when Reynolds number increases.

7. The BCCSVG show a high pressure drop than that of SCCSVG.

8. Good agreement was shown between the Numerical and Experimental studies in the present work.

9. Fluent program results show that VGs. can save energy of about 27% than that for the case of no VGs, where it can be increased by 96 W in order to have the same outlet conditions for the case of having VGs.

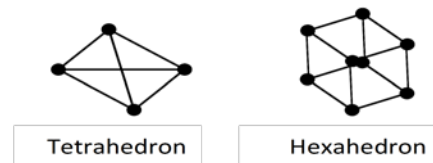
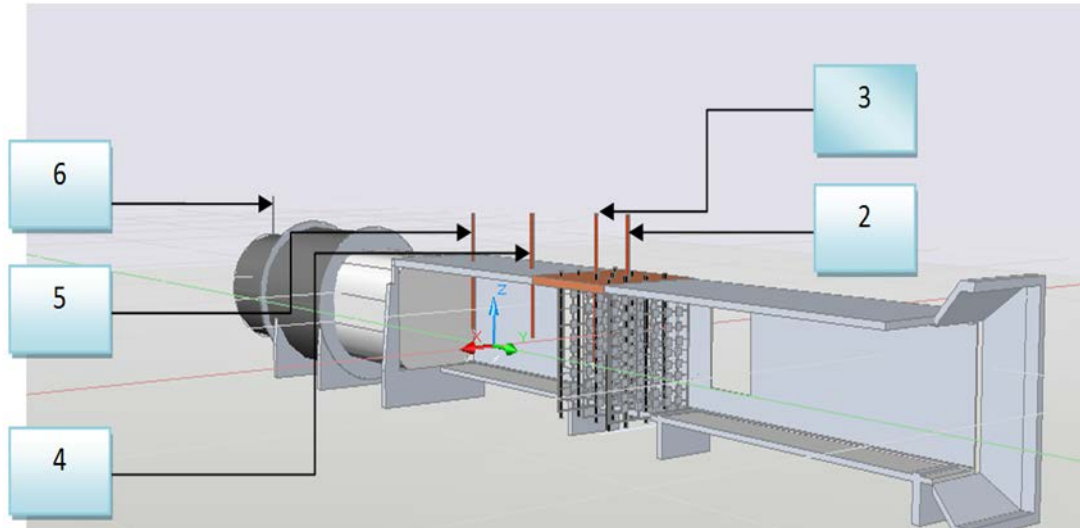


Figure 1 : Tetrahedron and hexahedron cells.



**Figure 2:** Rig with positions of thermocouples.

**Table 1:** shows the purpose of thermocouples' location that displayed in fig. (2)

Thermocouples number	Position	Thermocouples number	Position
1	To measure the ambient temperature	4	At 28 cm after last row of heaters
2	at 2.5 cm between first and second row of heaters	5	At 38 cm after last row of heaters
3	at 2.5 cm between second and third row of heaters	6	At the outlet of duct

**Table 2:** shows the purpose of thermocouples' location that displayed in fig. (2)

Thermocouples number	Position	Thermocouples number	Position
1	To measure the ambient temperature	4	At 28 cm after last row of heaters
2	at 2.5 cm between first and second row of heaters	5	At 38 cm after last row of heaters
3	at 2.5 cm between second and third row of heaters	6	At the outlet of duct



Figure (3-a): shows the VG. of SCCSVG type.



Figure (3-b): shows the VG. of BCCSVG type.

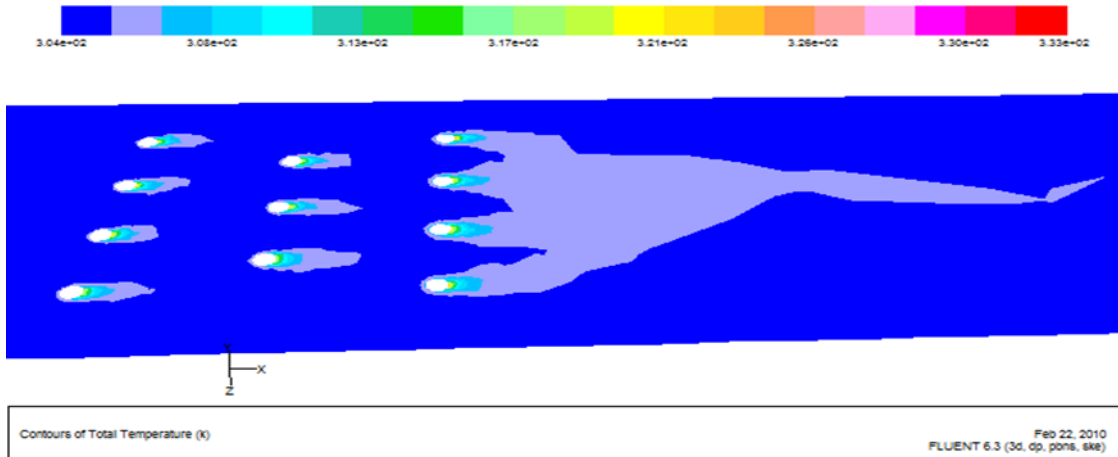


Figure (4) : The contour distribution of total temperature for the duct without VGs at velocity=4 m/s

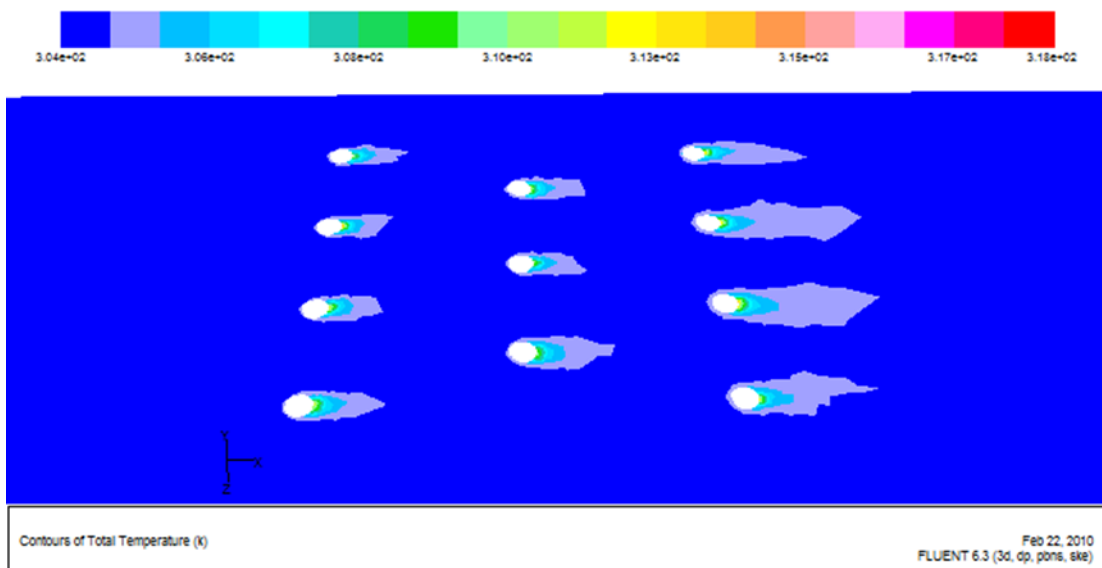
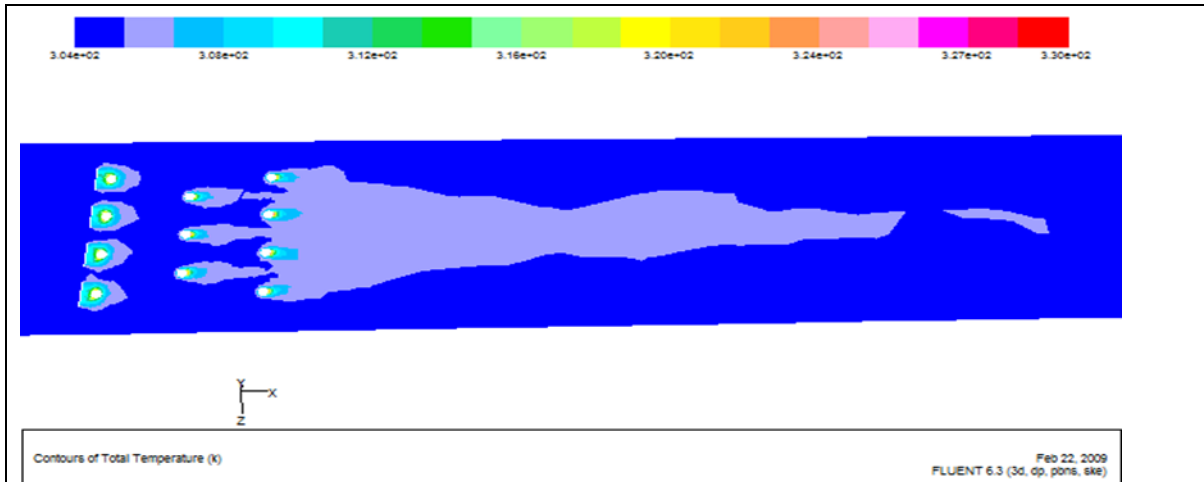
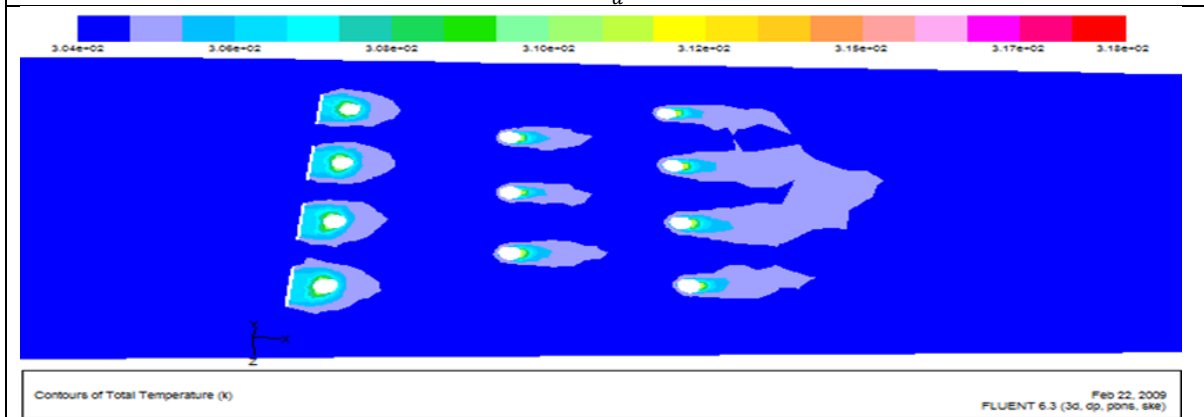


Figure (5) : The contour distribution of total temperature for the duct without VGs at velocity=10 m/s

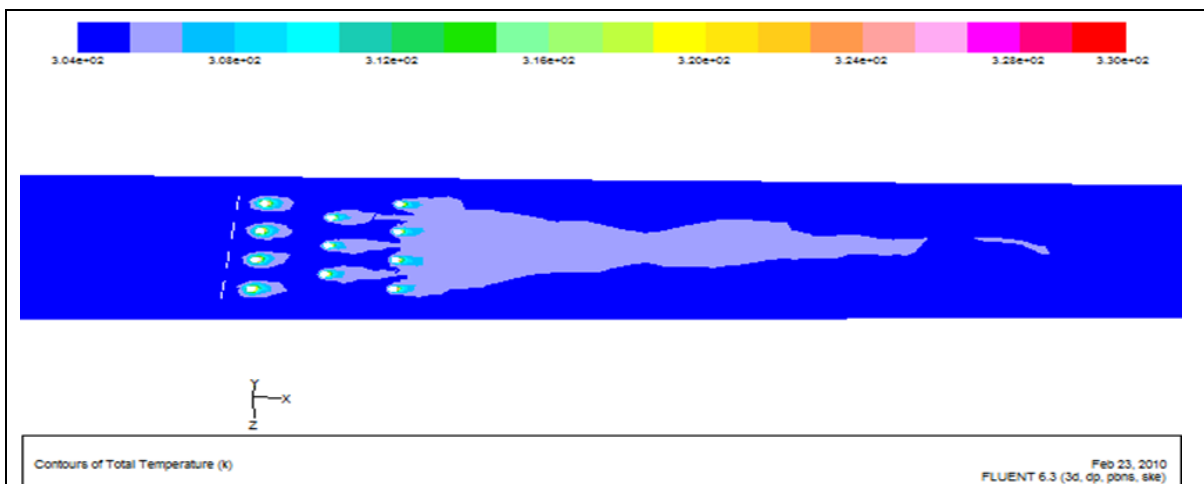




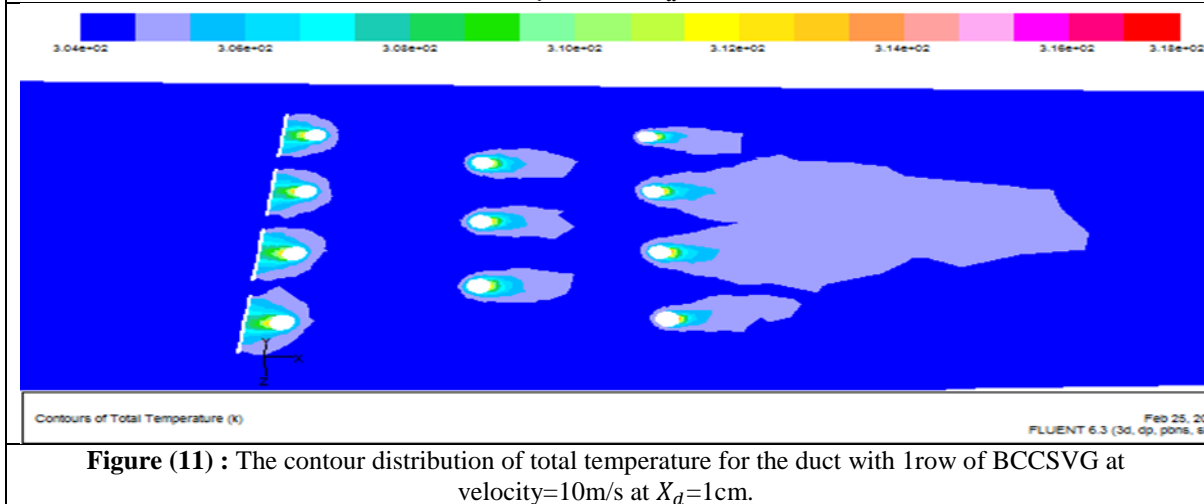
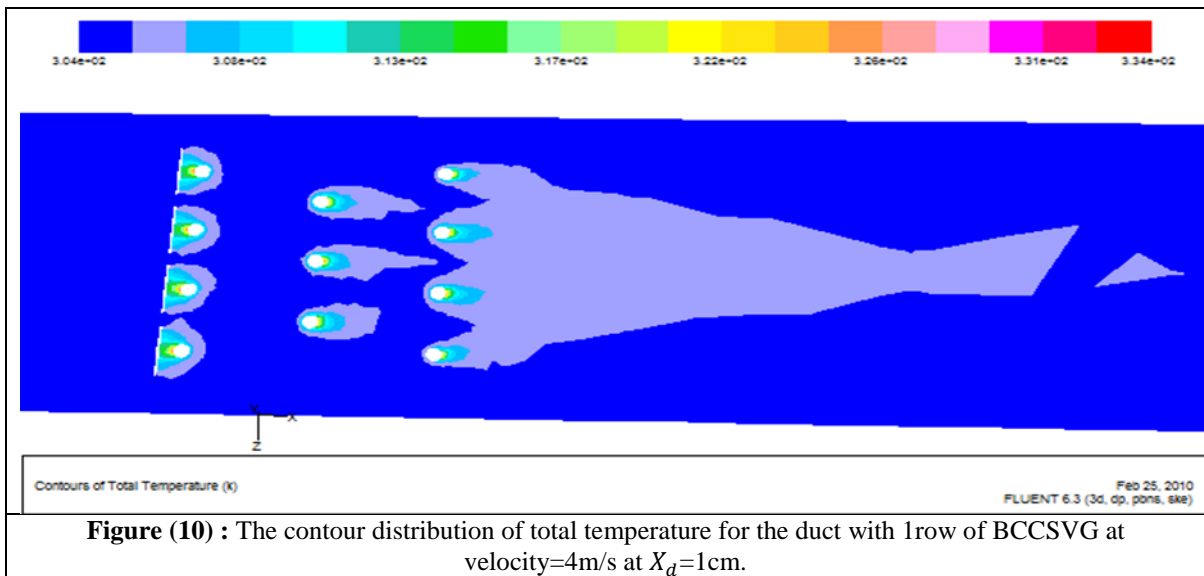
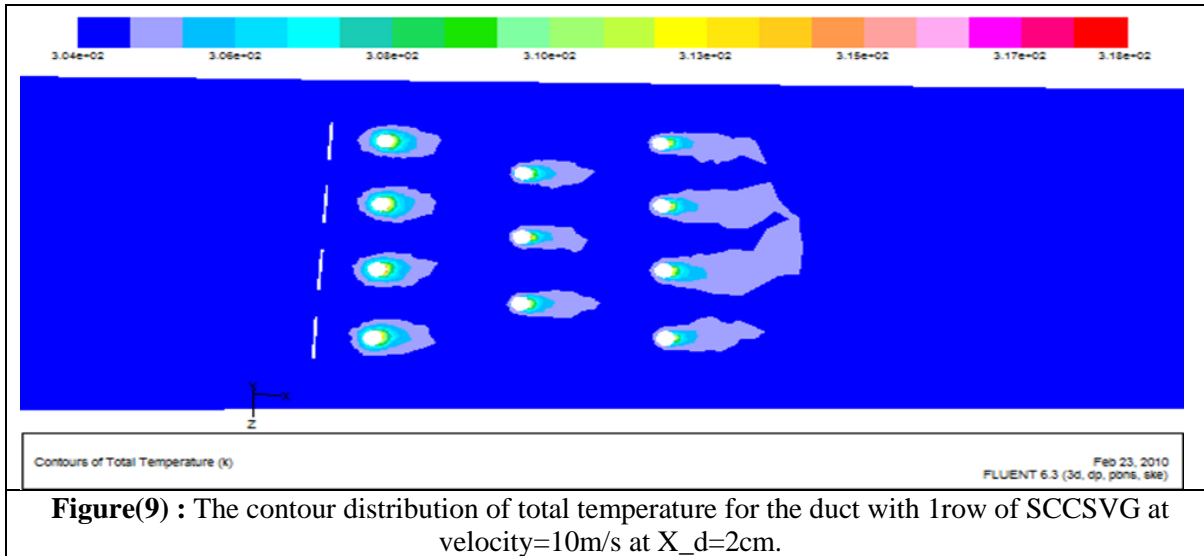
**Figure (6) :** The contour distribution of total temperature for the duct with 1row of SCCSVG at velocity=4 m/s at  $X_d=1$ cm



**Figure (7) :** The contour distribution of total temperature for the duct with 1row of SCCSVG at velocity=10m/s at  $X_d=1$ cm.



**Figure (8) :** The contour distribution of total temperature for the duct with 1row of SCCSVG at velocity=4m/s at  $X_d=2$ cm.



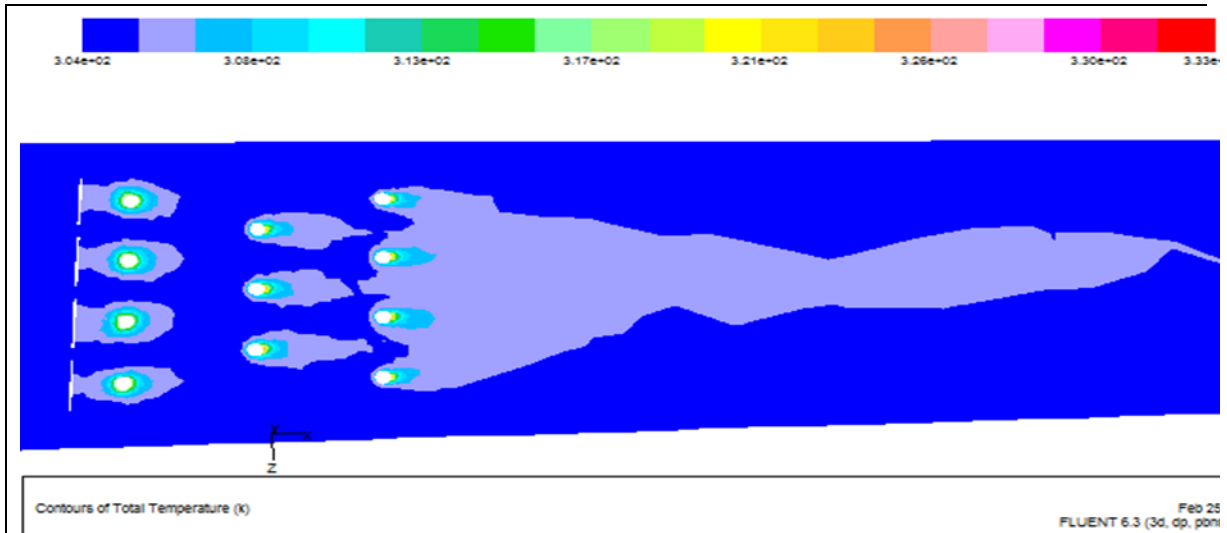


**Figure (12) :** The contour distribution of total temperature for the duct with 1row of BCCSVG at velocity=4m/s at  $X_d=2$ cm.

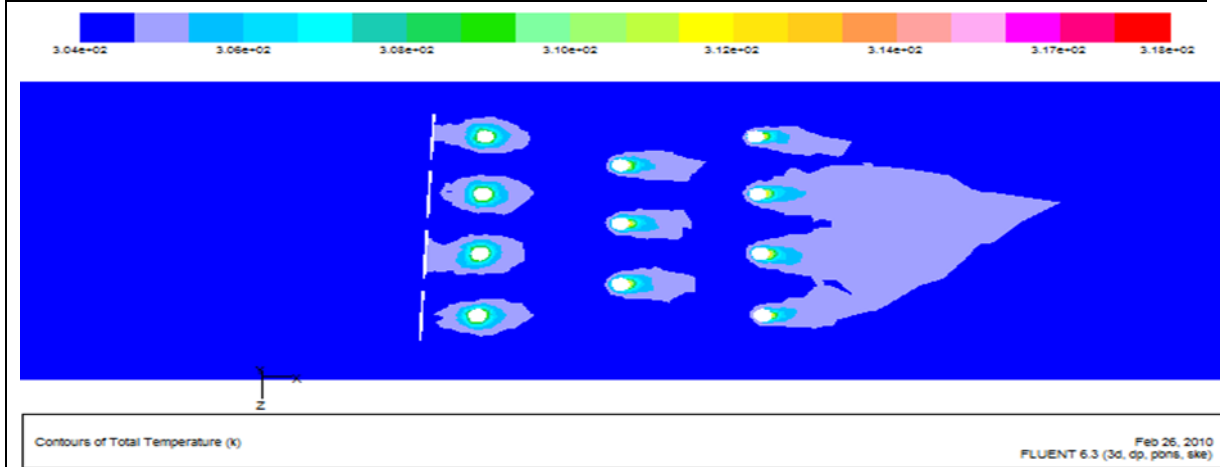


**Figure (13) :** The contour distribution of total temperature for the duct with 1row of BCCSVG at velocity=10m/s at  $X_d=2$ cm.

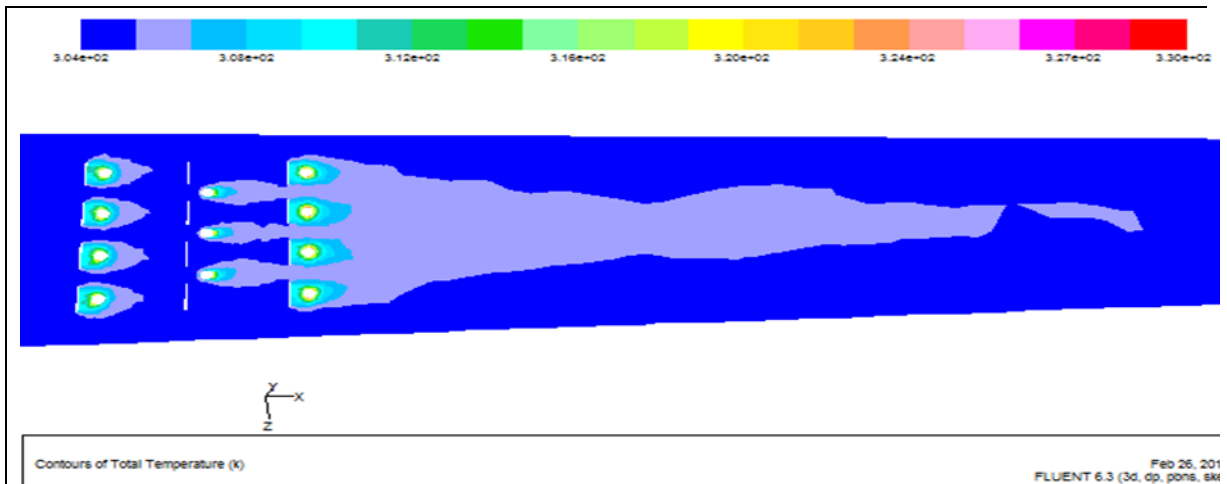


**Figure (14) :** The contour distribution of total temperature for the duct with 3rows of SCCSVG at velocity=4m/s at  $X_d=1$ cm.

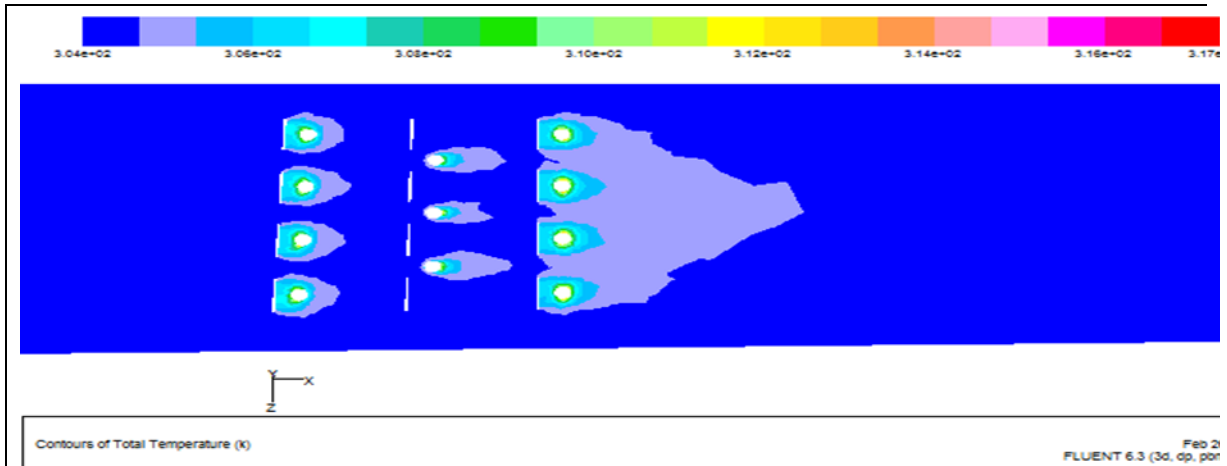


**Figure (15) :** The contour distribution of total temperature for the duct with 3rows of SCCSVG at velocity=10m/s at  $X_d=1$ cm.

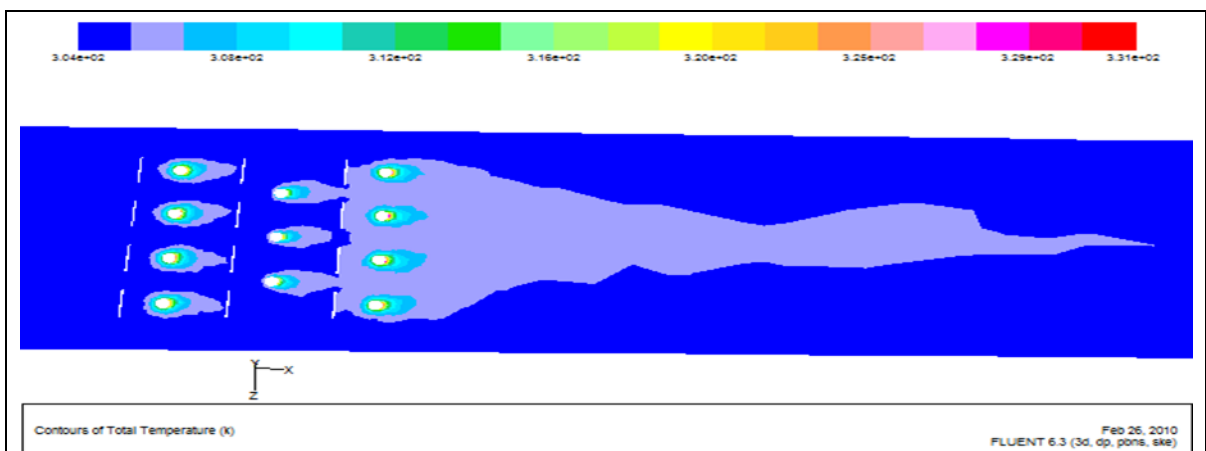


**Figure (16) :** The contour distribution of total temperature for the duct with 3rows of SCCSVG at velocity=4m/s at  $X_d=2$ cm.

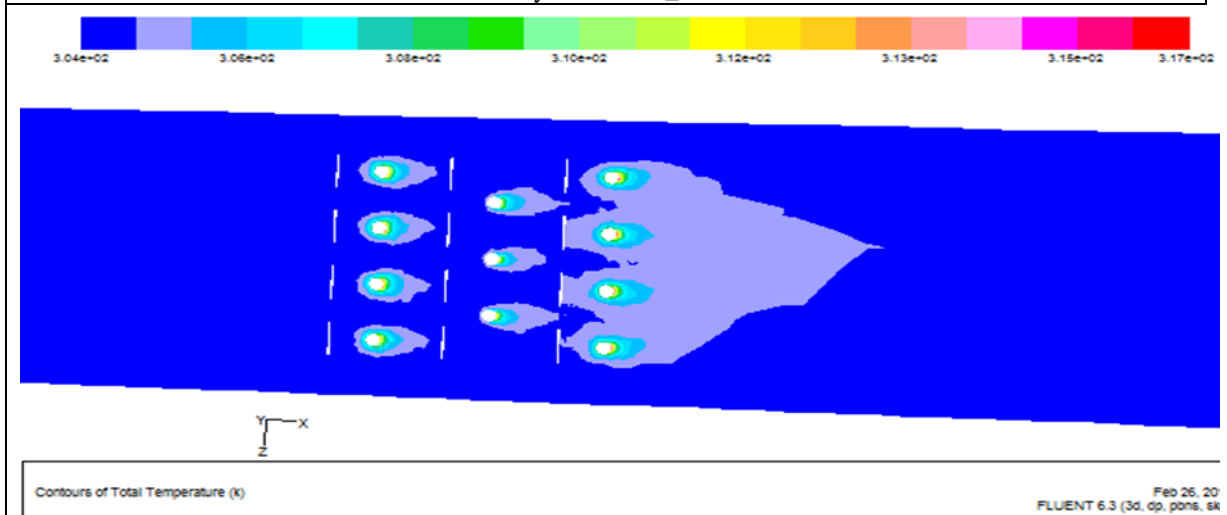


**Figure (17) :** The contour distribution of total temperature for the duct with 3rows of SCCSVG at velocity=10m/s at  $X_d=2$ cm.

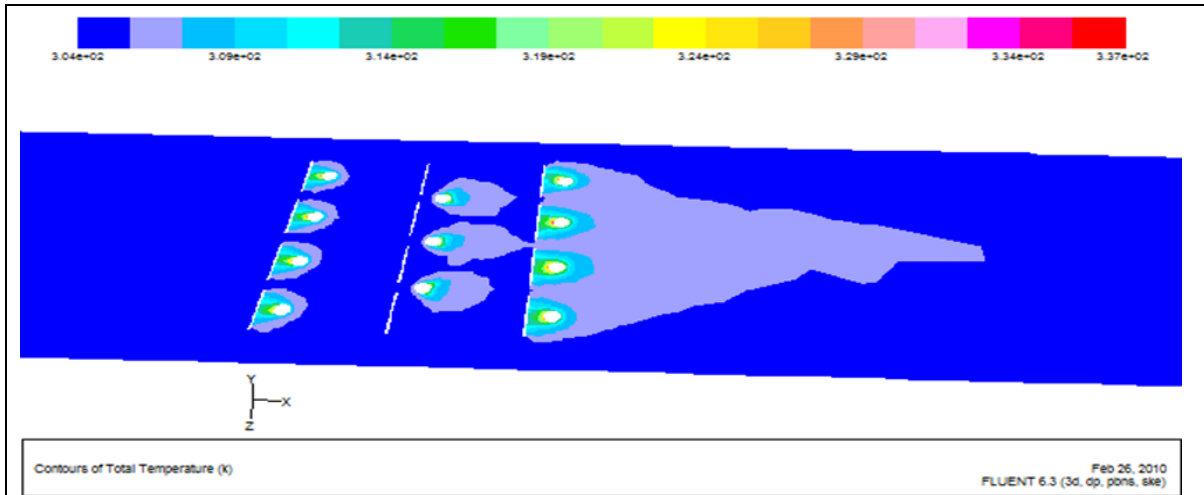


**Figure (18) :** The contour distribution of total temperature for the duct with 3rows of BCCSVG at velocity=4m/s at  $X_d=1$ cm.

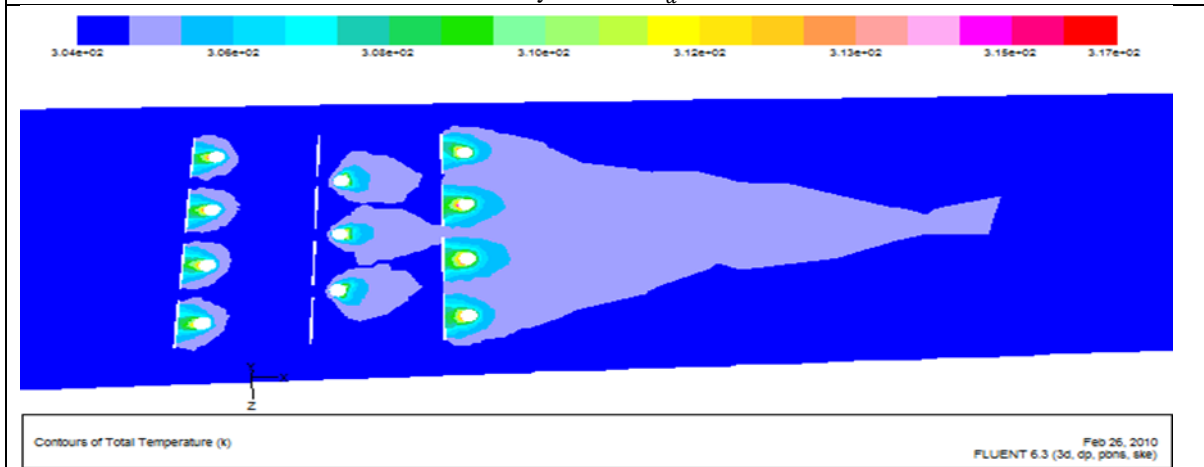


**Figure (19) :** The contour distribution of total temperature for the duct with 3rows of BCCSVG at velocity=10m/s at  $X_d=1$ cm.

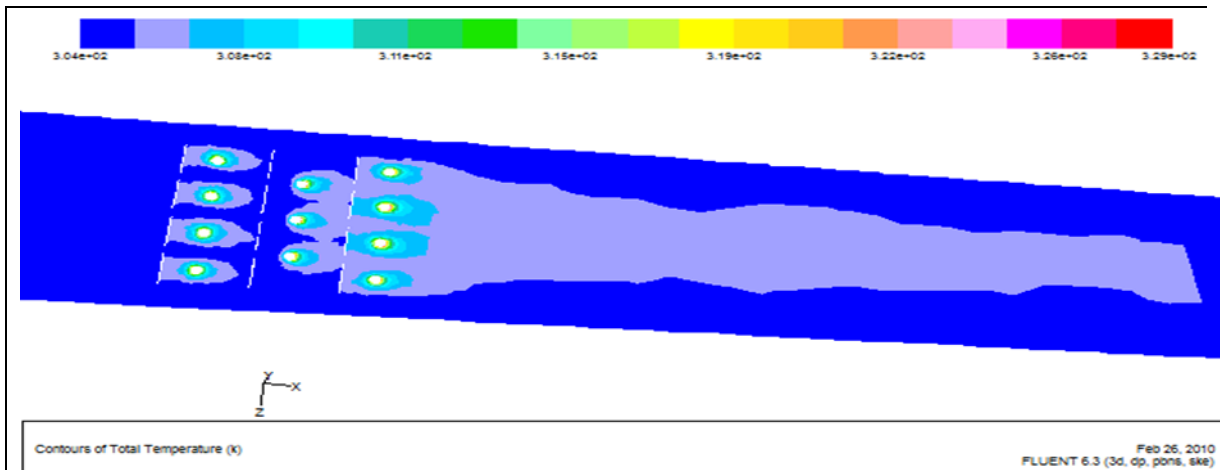


**Figure (20) :** The contour distribution of total temperature for the duct with 3rows of BCCSVG at velocity=4m/s at  $X_d=2$ cm.

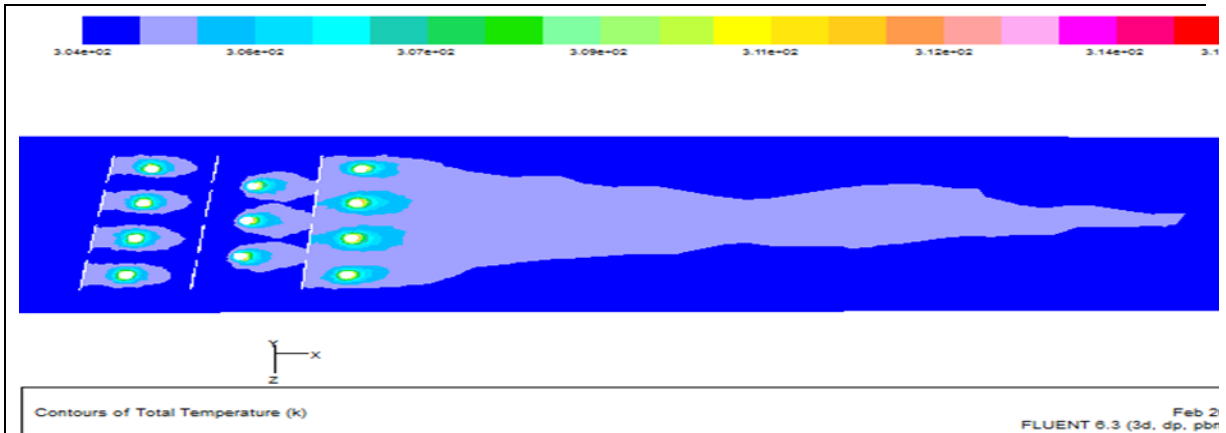


**Figure (21) :** The contour distribution of total temperature for the duct with 3rows of BCCSVG at velocity=10m/s at  $X_d=2$ cm.

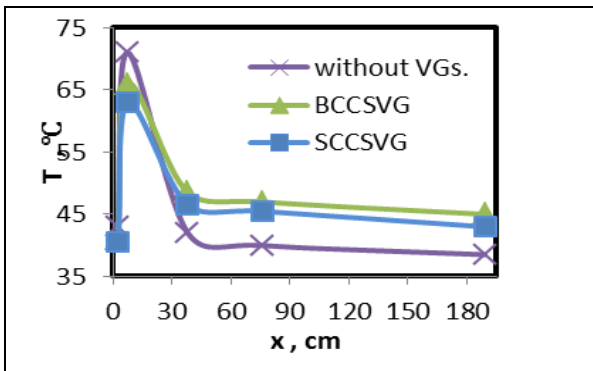


**Figure (22) :** Temperature distribution vs. duct length (x) to the duct with 1 row of VGs of  $X_d=1$  cm of 4m/s

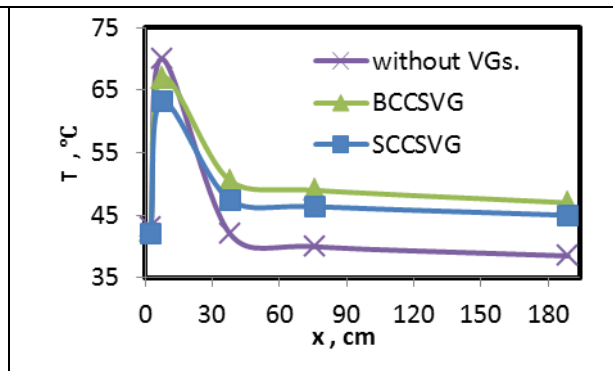


**Figure (23) :** Temperature distribution vs. duct length (x) to the duct with 1 row of VGs of  $X_d=2$  cm of 4 m/s

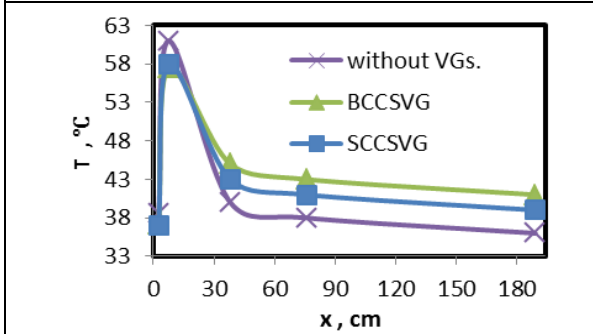


**Figure (24) :** Temperature distribution vs. duct length (x) to the duct with 1 row of VGs of  $X_d=1$  cm of 10 m/s

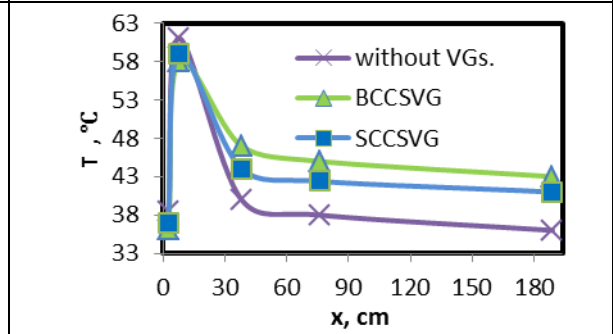


**Figure (25) :** Temperature distribution vs. duct length (x) to the duct with 1 row of VGs of  $X_d=2$  cm of 10 m/s

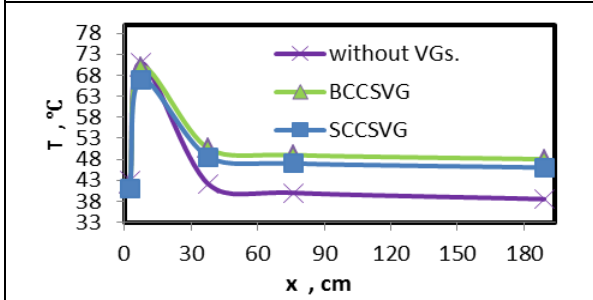


**Figure (26) :** Temperature distribution vs. duct length (x) to the duct with 3 rows of VGs of  $X_d=1$  cm of 4 m/s

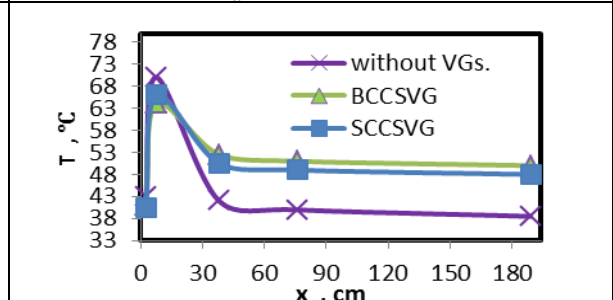


**Figure (27) :** Temperature distribution vs. duct length (x) to the duct with 3 rows of VGs of  $X_d=2$  cm of 4 m/s

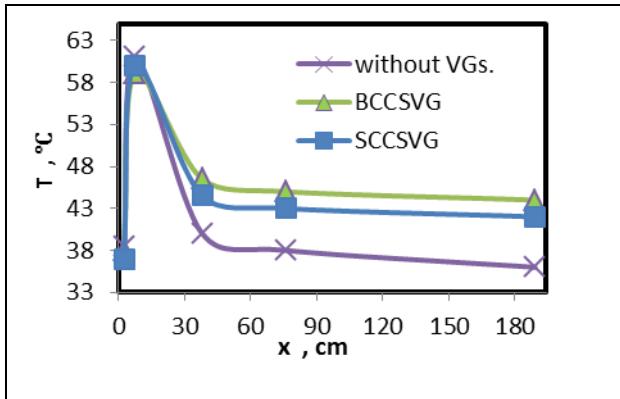


**Figure (28) :** Temperature distribution vs. duct length (x) to the duct with 3 rows of VGs of  $X_d=1$  cm of 10 m/s

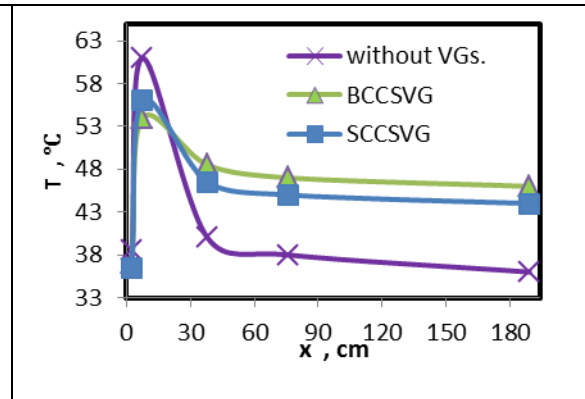


**Figure (29) :** Temperature distribution vs. duct length (x) to the duct with 3 rows of VGs of  $X_d=2$  cm of 10 m/s

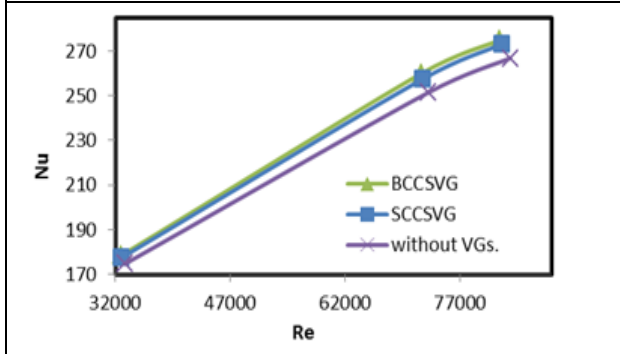


**Figure (30) :** Nusselt number vs. Reynolds number

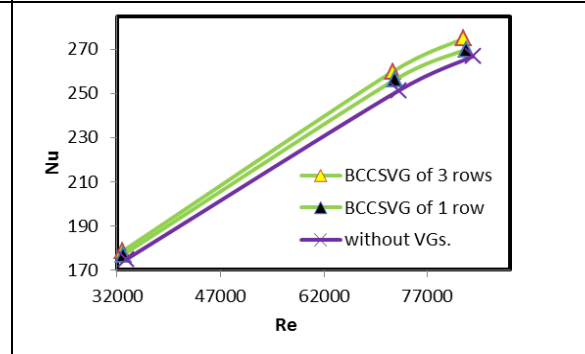


**Figure (31):** Nusselt number vs. Re to compare the 1 row and 3 rows of VGs at  $X_d=1$  cm

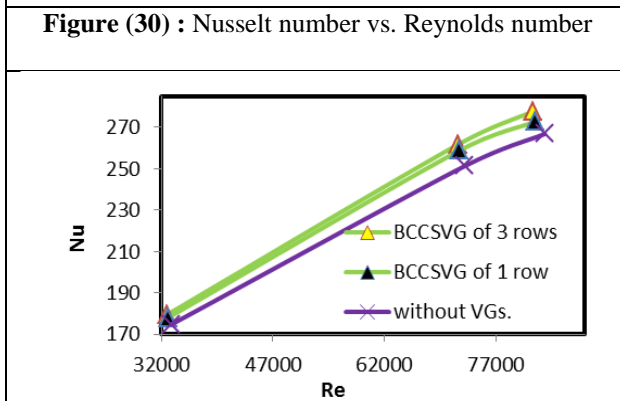


**Figure (32) :** Nusselt number vs. Re to compare the 1 row and 3 rows of VGs at  $X_d=2$  cm

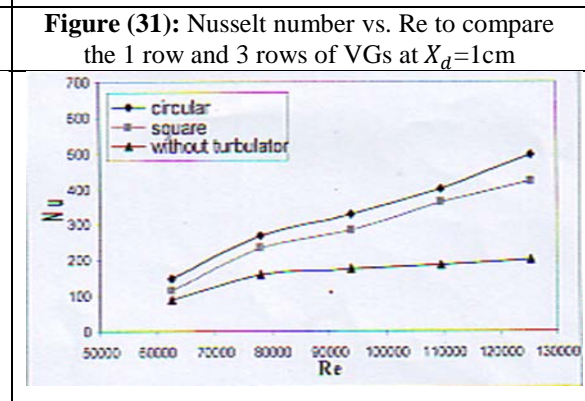


**Figure (33):** Experimental variation of Nusselt number with Reynolds number at location ( $X=1.5$  cm) for vortex generators [11].

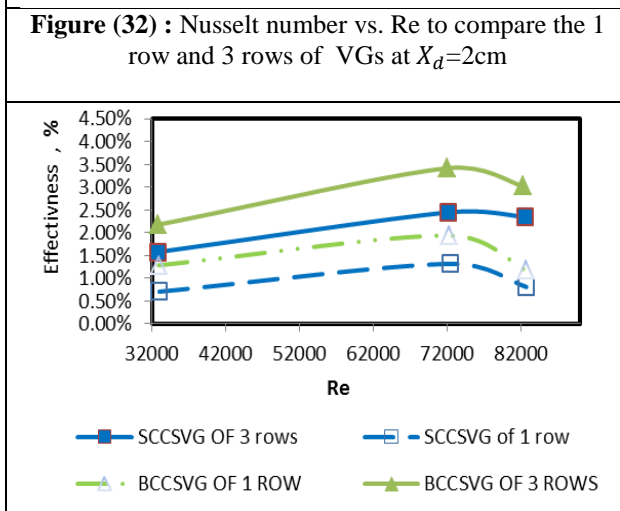


**Figure (34) :** Effectiveness vs. Re to compare the 1 row of VGs and 3 rows of VGs at  $X_d=1$  cm.

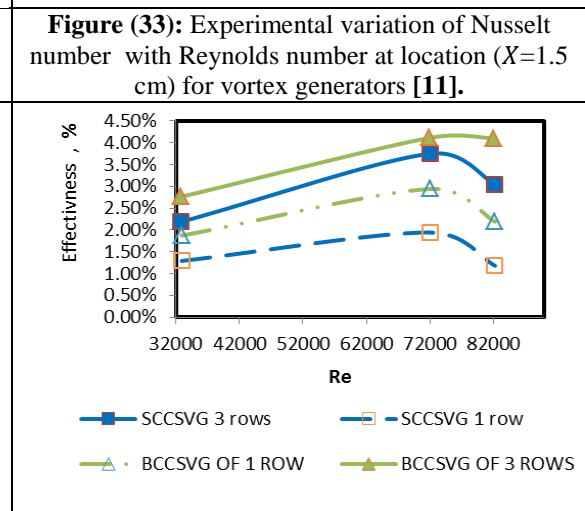


**Figure (35) :** Effectiveness vs. Re to compare the 1 row and 3 rows of VGs at  $X_d=2$  cm

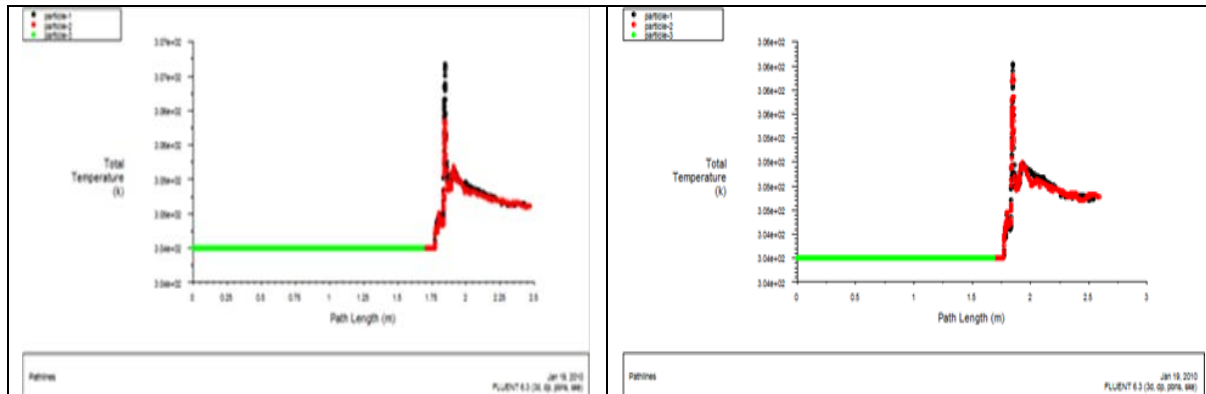


**Figure (36):** Total temperature with duct length for 3rows of BCCSVG at  $X_d=2$ cm.

**Figure (37):** Total temperature with duct length of 1rows of BCCSVG at  $X_d=2$ cm.

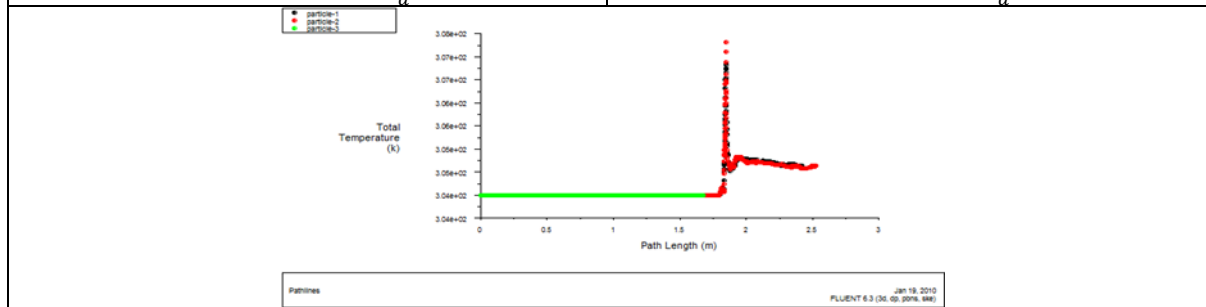


**Figure (38):** Total temperature with duct length for the case of without VGs.

**References**

[1] Hussain, A. A. (2005), “Experimental Study on Heat Transfer Enhancement in pipes Using Helical Wire Insert”, MSC Thesis, Mech. Eng. Dept., University Of Technology.

[2] Gentry, M. C. and Jacobi, A. M. (2002), “Heat Transfer Enhancement by Delta-Wing Generated Tip Vortices in Flat-Plate And Developing Channel Flows “, Transactions Of The ASME, Journal Of Heat Transfer, Vol.124, pp.1158-1168.

[3] Quintino, A. (2012), “Experimental analysis of the heat transfer coefficient enhancement for a heated cylinder in cross-flow downstream of a grid flow perturbation” , Applied Thermal Engineering , pp. 55-59.

[4] MANGLIK, R. M. ”HeatTransfer Enhancement”, chapter 14.pp. 1029-1130.

[5] O’Brien, J. E., Sohal, M.S., Foust, T. D. and Wallstedt, P. C. (2002) “Heat transfer enhancement for finned-tube heat exchangers with vortex generators: experimental and numerical results”, Idaho National Engineering and Environmental Laboratory (INEEL).

[6] Hiravennavar, S.R., Tulapurkara, E.G. and Biswas, G. (2007) “A note on the flow and heat transfer enhancement in a channel with built-in winglet pair”, International Journal of Heat and Fluid Flow ,Vol.28,pp. 299–305.

[7] epaiwa, N., Chompookham, T. and Promvonge, P. (2010) , “ Thermal enhancement in a solar air heater channel using rectangular winglet vortex generators ”, Proceedings of the International Conference on Energy and Sustainable, pp. 1-7.

[8] Wu, J.M. and Tao, W.Q. (2008) “ Numerical study on laminar convection heat transfer in a rectangular channel with longitudinal vortex generator.Part A: Verification of field synergy principle ”, International Journal of Heat and Mass Transfer , Vol. 51 , pp. 1179–1191.

[9] Min, C., Qi, C., Kong, X. and Dong, J. (2010) “Experimental study of rectangular channel with modified rectangular longitudinal vortex generators”, International Journal of Heat and Mass Transfer, Vol. 53, pp. 3023–3029.

[10] Holman, J.P. (2007), “Experimental Methods for Engineers”, Seventh Edition. Michigan University. McGraw-Hill, 1971. pp.423.

[11] Kattea, W.A., (2012), “An Experimental Study On The Effect Of Shape And Location Of Vortex Generators Ahead Of A Heat Exchanger”, Al-Khawarizmi Engineering Journal, Vol.8, pp. 12-29.



## محاكاة نظرية وعملية لتأثير المساحات لمولدات الدوامات على تحسين انتقال الحرارة في مجرى في داخلة مسخنات كهربائية

فتية جميل الخشالي  
هندسة المكنائ و المعدات  
جامعة فيلادلفيا  
عمان- الاردن

افراح تركي عواد  
طالبة دكتوراة في قسم الهندسة الميكانيكية  
جامعه ليدز  
ليدز- المملكة المتحدة

### الخلاصة :

اجريت محاكاة نظرية و عددية لمعرفة تأثير المساحات المختلفة لمولدات دوامات (شبكة دوائر صغيرة و شبكة دوائر كبيرة) على مجال الجريان و انتقال الحرارة من مجرى بداخله ملفات تسخين كهربائية و لقيم رينولدز مختلفة من 32000 الى 83000 مع ثبوت الفيض الحراري =43.09426 كيلو واط/م<sup>2</sup>. بالمحاكاة العددية تم استخدام برنامج الفلوننت (6,3) مع حلول بالفرضيات التالية : جريان مستقر و ثلاثي الابعاد وكذلك حل معادلات الاستمرارية, معادلات الزخم و معادلات الطاقة باستخدام نموذج (k-ε) القياسي. باستخدام برنامج الفلوننت تم استنتاج ان وجود مولدات الدوامات يحفظ الطاقة بمقدار 27% من طاقة المسخنات بتأثير زيادة مساحة مولدات الدوامات (كنسبة نصف قطر مولدات الدوامات ذات المقطع الدائري الكبير الى نصف قطر مولدات الدوامات ذات المقطع الدائري الصغير=1.5) ولفس الشكل على اداء المسخنات. النتائج العملية تبين انه هنالك تحسين بانتقال الحرارة بوجود مولدات الدوامات حيث يعتمد تحسين انتقال الحرارة على مساحه مولدات الدوامات و تبين ان ذات النوع الدائري الكبيره هي أفضل في تحسين انتقال الحراره بمقدار (2.76%-4.11%) في حالة وجود ثلاثة صفوف من مولدات الدوامات وعلى بعد 2سم قبل او بين المسخنات و مولدات الدوامات. ان الزيادة في: (مساحة مولدات الدوامات, عدد صفوف مولدات الدوامات , المسافة بين أي صفيين من مولدات الدوامات والمسخنات) هذه تعتبر اكثر العوامل المؤثرة على تحسين انتقال الحرارة.

**كلمات المفاتيح:** مولدات دوامات , انتقال الحرارة.